The Use of the Artificial Damped Outrigger Systems in Tall R.C Buildings Under Seismic Loading

Dr. Abbas Abd Elmajeed Allawi
Assistant Professor
College of Engineering - University of Baghdad
E-mail: abbasallawi2004@yahoo.com

Amneh Hamid Al Mukhtar
M. Sc. Student
College of Engineering - University of Baghdad
E-mail: amena1981eng@gmail.com

ABSTRACT

This paper studies the combination of fluid viscous dampers in the outrigger system to add supplementary damping into the structure, which purpose to remove the dependability of the structure to lower variable intrinsic damping. This optimizes the accuracy of the dynamic response and by providing higher level of damping, basically minimizes the wanted stiffness of the structure while at the same time optimizing the achievement.

The modal considered is a **36** storey square high rise reinforced concrete building. By constructing a discrete lumped mass model and using frequency-based response function, two systems of dampers, parallel and series systems are studied. The maximum lateral load at the top of the building is calculated, and this load will be applied at every floor of the building, giving a conservative solution. For dynamic study **Response Spectrum Analysis** was conducted and the behavior of the building was determined considering response parameters. **MATLAB** software, has been used in the dynamic analysis for three modes.

For all modes, it is observed that the parallel system of dampers result in lower amplitude of vibration and achieved more efficiently compared to the damper is in series, until the parallel system arrives **100%** damping for mode three.

Key words: outrigger system, fluid viscous damper, discrete model.

استخدام أنظمة دعامة الإخماد الاصطناعي في المباني الخرسانية المسلحة العالية تحت تأثير الأحمال الزلزالية

د. عباس عبد المجيد علاوي
استاذ مساعد
كلية الهندسة-جامعة بغداد

آمنة حامد المختار
طالبة ماجستير
كلية الهندسة-جامعة بغداد

الخلاصة

تمت دراسة عملية دمج مخمدات السائل اللزج في نظام الدعامة لإضافة إخماد تكميلي للمنشأ ، والذي يهدف إلى إزالة اعتماد المنشأ على القيمة المنخفضة للإخماد الجوهري. هذا يحسن من دقة الاستجابة الديناميكية ومن خلال توفير مستوى أعلى من التخميد، بشكل أساسي يتم تقليل الصلابة المطلوبة للمنشأ في الوقت نفسه يتم تحسن الأداء.

النموذج الذي اخذ بنظر الاعتبار لهذه الدراسة هو 36 طابق مربع المقطع للمباني الخرسانية المسلحة الشاهقة. من خلال انشاء نموذج من كتل متجمعة منفصلة, واستعمال دالة الاستجابة المعتمدة على التردد, لنظامين من المخمدات، وهما نظاما التوازي والتوالي ويتم دراستها. يتم احتساب الحد الأقصى للحمل الجانبي في الجزء العلوي من المبنى، وسيتم تطبيق هذا الحمل في كل طابق من المبنى، معطيا حلا محافظا. للحالة الديناميكية يتم استعمال طريقة استجابة تحليل الطيف ويتم تحديد سلوك المبنى بالاخذ بنظر الاعتبار لمتغيرات الاستجابة. برنامج MATLAB, استعمل في التحليل الديناميكي لثلاثة انماط.

لكل الانماط، لوحظ أن المخمد السائل اللزج بوضعية التوازي ينتج ذبذبات ذات قيم اقل ويحقق كفاءة أكثر مقارنة عندما المخمد بوضعية التوالي. حتى يصل لنظام التوازي الى الاخماد بنسبة 100٪ للنمط الثالث.

الكلمات الرئيسية: نظام الدعامة, مخمد السائل اللزج, نموذج منفصل.

1. INTRODUCTION

Outrigger are a common system of strengthening and stiffening tall buildings. They work by connecting the central core, comprising either braced frames or shear walls, to the outer perimeter columns. The explication of building outrigger behavior is easy because outriggers represent as firm arms engaging external columns, at the point when a core have a tries to incline, its rotation at the outrigger level generates a tension- compression couple in the external column moving contrary to that movement. As the outcome, the outrigger restrict the bending of the core by introducing a point of inflection in the deflection profile, as shown in **Fig.1**. Thus decreasing the lateral motion at the top when the reversal in curvature**, Nanduri, et al., 2013** and **Melek, et al., 2012.**

Besides at the outrigger intersection lowering the core moment, the system equals the differential shortening of exterior columns coming from axial load imponderables and temperature. Another influence of using outriggers is the considerable lowering of net tension and uplift force at the foundation level**, Choi, et al., 2012.**

The damped outrigger system works by the insertion of viscous dampers between the external columns and the outriggers. When it done, there was a considerable rise in damping**, Willford,** and **Simith, 2008.** Therefore, the outrigger system is used as one of the structural system to control the excessive drift during lateral load due to earthquake load.

2. STRUCTURAL DESCRIPTION AND MODELING

2.1 Structural Parameters

The modal considered for this study is 36 stories square high rise reinforced concrete building with a base dimension of 30 m by 30 m will be analyzed. The floor to floor height is 4 m contributing to a total building height of 144 m. The building will have a 14 m by 14 m central concrete core with a thickness of 45 cm. The building will have two outrigger arms cantilevering from the core to the perimeter columns from each of the side of the core. W14**X**398 sections with an approximate cross-section area of 0.15 m^2 will be utilized as the perimeter columns**, Gamaliel, 2008** and **Smith** and **Willford, 2007.**

The gravity system used in conjunction with central concrete core consists of 25 cm thick reinforced concrete slabs, with beams section of 45 cm **X** 70 cm, and square reinforced concrete columns (45 cm **X** 45 cm). Fig. 2 summarizes the building dimensions described.

2.2 Structural Model

To create a realistic modal of the proposed building described in section 2.1, each floor of the building will be modeled as a series of masses lumped at the center of the core. Each mass will have three degrees of freedom and the vertical translation degree of freedom has been neglected to simplify the modal, as shown in **Fig. 3**.

The general discrete equation of motion written in matrix form as

$$\boldsymbol{M\,\ddot{U} + C\,\dot{U} + K\,U = P} \tag{1}$$

To obtain the global stiffness matrix, the direct stiffness approach is used. A standard two-node member element with two degrees of freedom for each node is considered in this study. The element stiffness matrix are given by

$$\boldsymbol{k(n)_{AA}} = \begin{bmatrix} \left(\frac{AE}{L}\,(sin\,a)^2 + \frac{12EI}{L^3}\,(cos\,a)^2\right) & \frac{6EI}{L^2}\,cos\,a \\ \frac{6EI}{L^2}\,cos\,a & \frac{4EI}{L} \end{bmatrix} \tag{2}$$

$$\boldsymbol{k(n)_{AB}} = \begin{bmatrix} \left(-\frac{\boldsymbol{AE}}{\boldsymbol{L}}\,(\boldsymbol{sin\,a})^2 + \frac{\boldsymbol{12EI}}{\boldsymbol{L^3}}\,(\boldsymbol{cos\,a})^2\right) & \frac{\boldsymbol{6EI}}{\boldsymbol{L^2}}\,\boldsymbol{cos\,a} \\ -\frac{\boldsymbol{6EI}}{\boldsymbol{L^2}}\,\boldsymbol{cos\,a} & \frac{\boldsymbol{2EI}}{\boldsymbol{L}} \end{bmatrix} \quad (3)$$

$$\boldsymbol{k(n)_{BA}} = \begin{bmatrix} \left(-\frac{\boldsymbol{AE}}{\boldsymbol{L}}\,(\boldsymbol{sin\,a})^2 + \frac{\boldsymbol{12EI}}{\boldsymbol{L^3}}\,(\boldsymbol{cos\,a})^2\right) & -\frac{\boldsymbol{6EI}}{\boldsymbol{L^2}}\,\boldsymbol{cos\,a} \\ \frac{\boldsymbol{6EI}}{\boldsymbol{L^2}}\,\boldsymbol{cos\,a} & \frac{\boldsymbol{2EI}}{\boldsymbol{L}} \end{bmatrix} \quad (4)$$

$$\boldsymbol{k(n)_{BB}} = \begin{bmatrix} \left(\frac{\boldsymbol{AE}}{\boldsymbol{L}}\,(\boldsymbol{sin\,a})^2 + \frac{\boldsymbol{12EI}}{\boldsymbol{L^3}}\,(\boldsymbol{cos\,a})^2\right) & -\frac{\boldsymbol{6EI}}{\boldsymbol{L^2}}\,\boldsymbol{cos\,a} \\ -\frac{\boldsymbol{6EI}}{\boldsymbol{L^2}}\,\boldsymbol{cos\,a} & \frac{\boldsymbol{4EI}}{\boldsymbol{L}} \end{bmatrix} \quad (5)$$

Where, A = area of the lumped mass = 53.19 m^2, E = elastic modulus of the core, I = moment of inertia of the lumped mass with respect to the bending axis $= 3184.406$ m^4, L = floor height = 4 m, a = angle of reference with respect to the global coordinate = 0, b = core length = 14 m, and t = core thickness = 0.45 m.

The mass matrix $\boldsymbol{M}$ is a diagonal matrix containing the floor mass as well as the rotational inertia of the following form

$$\boldsymbol{M} = \begin{bmatrix} \boldsymbol{M_1} & & & \boldsymbol{0} \\ & \boldsymbol{J_1} & & \\ & & \ddots & \\ & & & \boldsymbol{M_{36}} \\ \boldsymbol{0} & & & \boldsymbol{J_{36}} \end{bmatrix} \quad (6)$$

Since the floor layout is the same throughout the building height, $M_1 = M_2 = \cdots = M_{36} = M$. Similarly, the rotational inertia entries are equal throughout the height, thus $J_1 = J_2 = \cdots = J_{36} = J$. Rotational inertia is assumed to be provided by the concrete core system only, and the gravity system have negligible effect on rotation because it is not rigidly attached to the core**, Gamaliel, 2008**.

Where, M = nodal mass = gravity system mass (m_f) + core mass (m_c) = 1,100,093 Kg;
J= nodal rotational inertia = 7,895,042.64 Kg m^2.

The intrinsic damping in a high-rise building is a key design parameter. Although the effect of damping is less important for seismic response than for wind response, the values assigned to structural damping should be selected with care. The intrinsic damping ratio of between 1% and 2% appears reasonable for buildings more than 50 m and less than 250 m in height, **Willford, et al., 2008**. While some studies using the intrinsic damping ratio of **2.5%** for **50** stories high rise reinforced concrete building**, Melek, et al., 2012.**

2.3 The Damped Outrigger Concept

The concept of the damped outrigger is shown in **Figs. 4,5, and 6**. **Fig. 4** appears how the outrigger systems activate in easy conditions while incorporated inside a usual core-to-perimeter columns outrigger systems. As a structure subjects dynamic sway motion, there is proportional vertical motion between the ends of stiff outrigger element that cantilevering from the core and the perimeter column. There are needful for the outriggers to shift vertically proportional to the floor at these levels, while the floors bend in double curvature to stay attached to the outer columns and the central core. The dampers are incorporated across this building discontinuity, dissipating energy through the cyclic motion, and producing the raise in the total damping for the structure. **Fig. 5** shows in terms of a conceptually the form of detail commonly wanted at the level where the damper is incorporated. The arranging can be as shown in **Fig. 6** at the outriggers level in this situation, **Smith** and **Willford, 2007**.

2.4 The Damped Outrigger Model

While the concept given by **Willford** and **Smith** implies that the perimeter columns is in series configuration with the dampers. Parallel configuration of columns and dampers studied by **Gamaliel, 2008** provided a good comparative study, as shown in **Fig. 7.**

The approach to drive typical damper characteristic is based on macroscopic point of view. Where in this point of view, the stiffness is defined based on the slope of the diagonal line of the hysteresis loop and the damping is derived from the hysteresis loop of tested damper**, Al Mallah, 2011**. Then, the equivalent complex stiffness for both parallel and series configuration were obtain.

2.4.1 **Hysteresis loop and characteristics of tested damper**

Considering a simple single degree of freedom (**SDF**) system with a viscous damper is subjected to a harmonic load, under steady- state response, the damping force equals to:

$$\boldsymbol{P(t) = C_o \frac{du}{dt} = C_o\, \omega\, u_o\, cos(\omega t - \delta) = C_o\, \omega \sqrt{u_o^2 - u_o^2\, sin^2(\omega t - \delta)}}$$

$$\boldsymbol{= C_o\, \omega \sqrt{u_o^2 - [u(t)]^2}} \quad (7)$$

$$\boldsymbol{\left(\frac{u}{u_o}\right)^2 + \left(\frac{P(t)}{C_o\, \omega\, u_o}\right)^2 = 1} \quad (8)$$

Which is the equation of the ellipse shown in **Fig. 8.** The area enclosed by the ellipse is $\boldsymbol{\pi\,(u_o)(C_o\, \omega\, u_o) = \pi\, C_o\, \omega\, u_o^2}$, which is equal to the dissipated energy

$$\boldsymbol{E_D = 2\pi\, \zeta\, \frac{\omega}{\omega_n}\, K\, u_o^2} \quad (9)$$

Due to harmonic force with $\omega = \omega_n$, and based on macroscopic point of view, the loose stiffness, K_2 is defined based on the slope of the diagonal line of the hysteresis loop. The damping coefficient, C_o, is equal to the loose stiffness divided by ω, and is also calculated from above as:

$$\boldsymbol{C_o = \frac{E_D}{\pi \omega\, u_o^2}} \quad (10)$$

The equivalent damping ratio $\boldsymbol{\zeta_{eq}}$ calculated from a test at $\boldsymbol{\omega = \omega_n}$ would not be right at any exciting frequency, but it would be a satisfying approximation.

$$\boldsymbol{\zeta_{eq}} = \frac{\mathbf{1}}{\mathbf{4\pi}} \frac{\boldsymbol{E_D}}{\boldsymbol{E_{SO}}} \tag{11}$$

Where the strain energy, $E_{SO} = K\, u_o^2\ /2$ *is calculated from the stiffness K resolved by experience,* **Chopra, 2008**. Based on the above, C_o and ζ_{eq} can be calculated from hysteresis loop of the tested dampers.

The model considered for this study is based on the material behavior in linear elastic range. However, it must be mentioned that most dampers classified as viscous dampers do not behave fully linear over the range of the entire velocity. This due to nonlinear material behavior and sealing friction which ends up in a nonlinear viscous behavior at low velocities.

2.4.2 Derivation of equivalent complex stiffness

Damping introduces complexity to the solution by adding a term involving velocity. In order to define the complex frequency-response function, the steady-state motion of a **SDOF** system is applied for both parallel and series configuration, which the equivalent complex stiffness can be derived as:

- Parallel configuration, The harmonic motion at the forcing frequency, $\boldsymbol{\omega}$, can be expressed as

$$\boldsymbol{u(t) = H_u(\omega)\, e^{i\omega t}} \tag{12}$$

$$\boldsymbol{\dot{u}(t) = i\omega\, H_u(\omega)\, e^{i\omega t}} \tag{13}$$

The equation of motion for the parallel configuration of damper and column is

$$\boldsymbol{p(t) = k_{col}\, u(t) + C\, \dot{u}(t) = (k_{col} + i\omega C)\, H_u(\omega) = k_{eq}\, H_u(\omega)} \tag{14}$$

$$\boldsymbol{\therefore k_{eq} = k_{col} + i\omega C} \tag{15}$$

, Chopra, 2008 and **Gamaliel, 2008**, see **Fig**. **9**.

-Series configuration and the harmonic motion at the forcing frequency, $\boldsymbol{\omega}$, can be expressed as:-

$$\boldsymbol{u(t) = H_u(\omega)\, e^{i\omega t}\ , and\ u(t)_1 = H_{u1}(\omega)\, e^{i\omega t}} \tag{16}$$

$$\boldsymbol{\dot{u}(t) = H_u(\omega)\, e^{i\omega t}, and\ \dot{u}(t)_1 = i\omega\, H_{u1}(\omega)\, e^{i\omega t}} \tag{17}$$

Then, the equation for the series configuration of damper and column is

$$\boldsymbol{p(t) = k_{col}\, u(t)_1 = C\ (\dot{u}(t) - \dot{u}(t)_1)} \tag{18}$$

$$\boldsymbol{(i\omega C)\, H_u(\omega) = (k_{col} + i\omega C)\, H_{u1}(\omega)} \tag{19}$$

$$\boldsymbol{H_{u1}(\omega) = \frac{i\omega C}{k_{col} + i\omega C}\ H_u(\omega)} \tag{20}$$

$$\boldsymbol{p(t) = \frac{k_{col}\, i\omega C}{k_{col} + i\omega C}\, H_u(\omega) = k_{eq}\, H_u(\omega)} \quad (21)$$

$$\boldsymbol{\therefore k_{eq} = \frac{k_{col}\, i\omega C}{k_{col} + i\omega C}} \quad (22)$$

Chopra, 2008 and **Gamaliel, 2008**, see **Fig**. **10**. The above procedure has been derived by the equivalent complex stiffness for both parallel and series damper configuration. The next step is to obtain the rotational stiffness at the outrigger level.

2.4.3 Derivation of the rotational stiffness

The column-restrained outriggers oppose the rotation of the core, when subjected to lateral loads, causing the moments and the lateral deflections in the core to be minimal than if the freestanding core alone resisted the loading. The exterior moment is now resisted not by bending of the core alone, but also by the axial compression and tension of the exterior column connected to the outrigger**, Taranath, 2010**.

The axial shortening and elongation of column is clearly equal to the rotation of the core multiplied by their particular distances from the exterior column to the center of the core. If the distance of the equivalent columns is d/2 from the central core, the axial distortion of the columns is then equal to βd/2, where β is the core rotation. Then the stiffness of the equivalent spring is studied for unit rotation of the core (i.e., β = 1), therefore the axial deformation of the equivalent columns is equalize to 1 × d/2 = d/2 units, **Taranath, 2010**. The next step was the derivation of the rotational stiffness.

The corresponding axial load is as following

$$\boldsymbol{p(t) = A\, E\, d/2\, (aH)} \quad (23)$$

$p(t)$ is the column axial load; A is the column area; E is the modulus of elasticity; d is the distance from the center of core to the exterior column; aH is the height at the outrigger level, see **Fig. 11**. Using the notion K_R for the rotational stiffness, and noticing that there are two equivalent columns, each situated at a distance from the core, we obtain

$$\boldsymbol{K_R = p(t) \times d/2 \times 2} \quad (24)$$

$$\boldsymbol{K_R = \frac{A\, E\, d^2}{2\, aH}} \quad (25)$$

The addition of rotational stiffness to the core at the outrigger level can be obtained as follows

$$\boldsymbol{M = p(t) \times d/2} \quad (26)$$

Where, $\boldsymbol{p(t) = k_{eq}\, H_u(\omega)}$, $\boldsymbol{H_u(\omega) = \frac{d}{2}\, \beta}$, and $\boldsymbol{M = K_R\, \beta}$

$$\boldsymbol{\therefore K_R = k_{eq} \left(\frac{d}{2}\right)^2} \quad (27)$$

2.5 Applying Outrigger Effect to Discrete Model

The effect of the outrigger can be modeled by introducing a minor change in the stiffness matrix. A rotational spring is to be added to the nodal point where the outrigger is located. Hence, the outrigger nodal point will have a modified rotational stiffness comprised of the existing rotational stiffness from the core (cantilever beam) and the rotational stiffness, K_R, from the outrigger. From previous section, the value of K_R has been derived. Because the Damping introduces complexity to the solution by adding a term involving velocity, the equivalent complex stiffness has been derived for both parallel and series damper configuration, and has been incorporated this effect into the stiffness matrix of the core**, Gamaliel, 2008** and **Taranath, 2010**.

In the case of a damped outrigger, the damping matrix, $\boldsymbol{C}$, is required to solve the full differential equation of motion. The conventional approach is to work in the real domain by constructing the damping matrix and introducing the damping coefficient $\boldsymbol{C_o}$ at the location corresponding to the rotation of the outrigger node. However, it is algebraically more convenient to work in the complex domain, by collapsing the $\boldsymbol{C}$ matrix altogether and lumping the effect of damping into the stiffness matrix, forming an equivalent complex stiffness matrix**, Gamaliel, 2008**, which had been obtained in section 2.4.1.

3. DYNAMIC ANALYSIS

3.1 Modal Analysis

In order to analyze the dynamic response of the structure due to seismic effect, the first step of the procedure is to perform Eigen-value analysis of the building with an offered elastic stiffness and mass in order that coincide its modal characteristics. The characteristics of special importance are the natural period of vibration of the buildings and modal shapes. Consequently, the Eigen-value problem can be solved from the relationship

$$\boldsymbol{k\,\phi = \omega^2\, M\,\phi} \tag{28}$$

Where ϕ, the eigenvectors, represent the mode shape and the Eigen-values correspond to ω^2; M, the mass matrix(see Sec. 2.2); k, the element stiffness matrix(see Sec. 2.2) plus the rotational stiffness, K_R which has been derived in Sec. 2.4.3. The modal period of vibration of the building can then be obtained by the following equation

$$\boldsymbol{T = \frac{2\pi}{\omega}} \tag{29}$$

Using **MATLAB** software for each series and parallel configuration, the frequencies, natural periods, and mode shapes of the first three modes will be obtained. For modal analysis the frequency and damper coefficient are set to zero, therefore the equivalent complex stiffness for parallel configuration equal to k_{col}(see Eq. 15) and for series configuration close to zero(see Eq. 22). **Table 1** summarizes the frequency and natural periods of the first three modes for series and parallel configuration, and **Fig. 12** shows mode shapes of series and parallel systems. The fundamental period for series and parallel configurations equal to 2.246 and 2.202, respectively.

3.2 Modal Response Spectrum Analysis

The ground motion risks that rely on the regional seismicity depending upon a list of basics. Then considered to be ingrained in building designed to **ASCE 7-05** the design ground motions are depend on the margin of a minimal bound evaluation versus collapse. Depend on

experiment this minimal bound has been believed in ground motion to be almost a factor of 1.5, **Taranath, 2005**. Subsequently, the design earthquake ground motion has been selected at a ground motion shaking level that is 1/1.5, which is equal to the 2/3 of the MCE ground motion.

ASCE 7-05 explains the **MCE** ground motion at short periods, *Ss*, in terms of the mapped values of the spectral response acceleration and also at 1 second, *S*1, for site class *B* for soft rock. these values may be gained from the map developed by **USGS**. The maps developed by **USGS** define sites of fault using both the probabilistic and deterministic proceedings, and contours of random horizontal acceleration values**, Taranath, 2005.**

In this study, the parameters ***Ss*** and ***S*1** determine from the major map developed by **USGS**, in Irvine, California for site class D, using an importance factor, I_E , is equal to 1 for the Occupancy Category II, and the effective seismic weight, Wx at each node is equal to 12,000 KN.

For service-level estimates, the **response spectrum analyses** which uses modal analyses to obtain building response will generally be used for linear dynamic analysis**, Willford, et al., 2008.**

The effective masses are multiplied by the acceleration coefficient, CS_m, to afford individual modal base shears by the following equations

$$\boldsymbol{V_m = CS_m\ W_m} \tag{30}$$

$$\boldsymbol{W_m = \frac{\left(\sum_{i=1}^{n} W_i\ \phi_{im}\right)^2}{\sum_{i=1}^{n} W_i\ \phi_{im}^2}} \tag{31}$$

Where, CS_m, is the coefficient of the modal seismic design; W_m, is the loads of the effective modal gravity; W_i, the portion of the total gravity load of the structure at level i; ϕ_{im}, displacement amplitude while shaking at ith level.

The distributing the base shear for each mode up the height of the structure as a set of equivalent lateral forces (proportional to the mode shape and mass distribution), by the following equations

$$\boldsymbol{F_m = Cx_m\ V_m} \tag{32}$$

$$\boldsymbol{Cx_m = \frac{W_x\ \phi_{xm}}{\sum_{i=1}^{n} W_i\ \phi_{im}}} \tag{33}$$

Where, Cx_m, is the vertical distribution factor at the mth mode in the xth level.

The values of, V_m and F_m, for series and parallel configurations are shown in **Table 2**.

3.3 Dynamic Analysis Using Software Program

To get the response function of the structure to seismic dynamic excitation, a complex periodic loading function will be applied in which

$$\boldsymbol{P_t = p(t)\ sin wt,} \text{ or } \boldsymbol{P_t = p(t)\ cos wt} \tag{34}$$

The term $\boldsymbol{P_t}$ can therefore be expressed as

$$\boldsymbol{P_t = p(t)\ e^{i\omega t}} \tag{35}$$

In order to determine the amplitude of vibration, the general equation of motion as following

$$\boldsymbol{M\,\ddot{u}(t) + k_{eq}\,u(t) = p(t)\;e^{i\omega t}} \quad (36)$$

The resulting displacement is then the real or imaginary part of the complex displacement, which it mentioned in sec. 2.4.2, $u(t) = H_u(\omega)\, e^{i\omega t}$.
Taking the time derivative of equation, we obtain

$$\boldsymbol{\dot{u}(t) = H_u(\omega)\, e^{i\omega t}}, \text{ and } \boldsymbol{\ddot{u}(t) = -\omega^2\, H_u(\omega)\, e^{i\omega t}} \quad (37)$$

Substituting Eq. (37) into the differential Eq. (36**)**, we get

$$\boldsymbol{(k_{eq} - \omega^2 M) H_u(\omega) = p(t)} \quad (38)$$

For simplifying, the quantity $\boldsymbol{\widehat{k_{eq}}}$ is defined as following

$$\boldsymbol{\widehat{k_{eq}} = (k_{eq} - \omega^2 M)} \quad (39)$$

The matrix equation is run in **MATLAB** to be solved is

$$\boldsymbol{\widehat{k_{eq}}\; H_u(\omega) = p(t)} \quad (40)$$

Therefore, the displacement matrix is defined as following

$$\boldsymbol{H_u(\omega) = \widehat{u(t)} = \widehat{k_{eq}}^{-1}\; p(t)} \quad (41)$$

For analysis purpose, the maximum drift at the top is used $\widehat{u(t)}_{36}$. The value k_{eq} is a complex quantity due to contribution from damping, see **Sec. 2.4.2** for series and parallel configuration. Therefore the resulting displacement contains the real and imaginary parts. Taking the sum of the squares of the real and imaginary parts to obtained the amplitude value, then taking the square root as following

$$\boldsymbol{\left|\widehat{u(t)}_{36}\right| = \sqrt{(\widehat{u(t)}_{36})^2_{real} + (\widehat{u(t)}_{36})^2_{imaginary}}} \quad (42)$$

The range of $\boldsymbol{\omega}$ is set to be from 0-55 rad⁄sec to cover the first three modes. The maximum equivalent lateral forces, which calculated in **Sec. 3.2**, applied at nodes at each modes.

Response function for series and parallel configuration at different values of damping coefficient at fundamental mode are shown in **Fig. 13**, it is observed that the parallel system of dampers result in lower amplitude of vibration compared to when the damper is in series and with increase of damping coefficient the fundamental frequencies of the building was raised for parallel system. Also, **Figs. 14, 15,** and **16**, show Frequency-based response function for the second and third modes, it is observed that the parallel placement of viscous damper result in lower amplitude of vibration compared to when the damper is in series, and see **Figs. 17** and **18** at constant frequency and natural periods of the first and second modes for difference values of damper coefficient.

3.4 Half Power Bandwidth Method

The half power bandwidth method employs the transfer function plot to get the damping. The method consists of deciding the frequencies at which the amplitude of the transfer function is $\mathbf{A_2}$ where

$$A_2 = \frac{A_{max}}{\sqrt{2}} \tag{43}$$

Where A_{max}, is the amplitude at the peak. The frequencies ω_1 and ω_2 associated with the half power points are obtained on either side of the peak, as shown in **Fig. 19**. Then the damping ratio $\boldsymbol{\xi}$ is getting employs the formula

$$\xi = \frac{\omega_2 - \omega_1}{2\omega_n} \tag{44}$$

The damping ratio associated with each natural frequency can be obtained using the half power bandwidth method.

To investigate the relationship between the amount of damping, response function were generated with different values of damping coefficient, **C**, and the corresponding fraction of critical damping, $\boldsymbol{\xi}$, is obtained by the half power bandwidth method in **MATLAB**.

The result of the relationship between the damping coefficient, **C**, and the critical damping, $\boldsymbol{\xi}$, is shown in **Table 3**.

4. CONCLUSIONS

- The use of complex stiffness matrix in dynamic analysis leading to a more efficient solution scheme and lumping the effect of damping into the stiffness matrix, forming an equivalent complex stiffness matrix, and has been incorporated this effect into the stiffness matrix of the core.
- For Eigen-value analysis, for the fundamental mode, the frequencies between the two configurations show a very slightly difference between series and parallel systems. Therefore, this slightly difference not appears in the plot. The frequencies to the higher modes (second and third) in both systems are obviously close to each other.
- For Frequency-based response function for mode one, it is observed that the parallel system of dampers result in lower amplitude of vibration compared to when the damper is in series. For series system, the critical damping reaches its peak at around ***C*** = **300,000** ***(KN.s/m)***, and beyond this point the critical damping loses its effectiveness gradually. While the parallel system increase of critical damping with increase of damping coefficient, and raising the fundamental frequencies of the building and has caused an increase in stiffness of the system and a decrease in fundamental period and become more narrow band of frequency as shown in **Fig. 13**.
- For Frequency-based response function for mode two, it is observed that resonant response occur over a very narrow band of frequency, which is very difficult to excite these modes continuously. But from analysis data, the parallel placement of viscous damper result in lower amplitude of vibration compared to when the damper is in series as shown in **Figs. 14 and 15**.
- For Frequency-based response function for mode three, it is observed that the critical damping is equal to **1.00**, which is **100%** damping for parallel system at any value of damping coefficient as shown in **Fig. 16(b)**.
- Both series and parallel systems will allow the reduction of member sizes and material due to the reduction of dynamic stiffness required. Viscous dampers can be made highly reliable

and redundant, eliminating the need to provide space for devices such as the tuned mass dampers. Damping applies to all frequency range. The structure as well as economic benefits of damped outrigger systems.

- The result of analysis suggests that viscous dampers should be installed in parallel with the perimeter column where the outrigger connects. However, to achieve this type of parallel connection takes more of a construction challenge than connecting it in line with column as proposed by **Smith** and **Willford,2007**. Two columns side by side will be required to connect the damper in parallel.

REFERENCES

- Al Mallah, N. M., 2011, *The Use of Bracing Dampers in Steel Building Under Seismic Loading*, Ms. D. Thesis : College of Engineering, University of Baghdad.

- ASCE, 2006, *ASCE Standard 7-05:Minimum Design Loads for Buildings and Other Structures* , American Society of Civil Engineers.

- Choi, H., Ho, G., Joseph, L., Mathias, N., 2012, *Outrigger Design for High Rise Buildings*, Chicago,USA : CTBUH Technical Guides.

- Chopra, A., 2008, *Dynamics of Structures:Theory and Applications to Earthquake Engineering*, New Delhi : Prentice-Hall of India.

- Gamaliel, R., 2008, *Frequency- Based Response of Damped Outrigger System for Tall Buildings*, Civil and Environmental Engineering, University of California.

- Melek, M., Darama, H., Gogus, A., and Kang, T., 2012, *Effects of Modeling of RC Flat Slabs on Nonlinear Response of High Rise Building Systems*, 15 WCEE.

- Nanduri, R., Suresh, B., and Hussain, I., 2013, *Optimum Position of Outrigger System for High- Rise Reinforced Concrete Buildings Under Wind and Earthquake Loadings*, American Journal of Engineering Research,Vol. 2, pp. 76- 89.

- Sathyanarayanan, K., Vijay, A., and Balachandar, S., 2012, *Feasibility Studies on the Use of Outrigger System for RC Core Frames*, India : Department of Civil Engineering, SRM University.

- Smith, R. J., and Willford, M. R., 2007, *The Damped Outrigger Concept for Tall Building*, Arup, London, UK : John Wiley & Sons, Inc.

- Taranath, B., 2010, *Reinforced Concrete Design of Tall Buildings*, US : Taylor and Francis Group.

- Taranath, B. S., 2005, *Wind and Earthquake Resistant Buildings: Structural Analysis and Design*, California : Marcel Dekken.

- Willford, M., and Simith, R., 2008, *Performance Based Seismic and Wind Engineering for 60 Story Twin Towers in Manila*, Beijing, China : The 14th World Conference on Earthquake Engineering.

➢ Willford, M., Whittaker, A., and Klemencic, R., 2008, *Recommendations for the Seismic Design of High- Rise Buildings*, Chicago : Council on Tall Buildings and Urban Habitat.

NOMENCLATURE

A = area of the lumped mass, m^2.
A_2=area of control valves, m^2.
A_{max}= amplitude at the peak, m.
aH=height at the outrigger level, m.
b = core length, m.
C_0= damping coefficient, N.s/m,
CS_m=modal seismic design coefficient, dimensionless.
Cx_m=vertical distribution factor at the *x*th level in the *m*th mode, dimensionless.
E =elastic modulus of the core, Pa.
E_D = energy dissipation, N.m.
E_{SO}= strain energy, N.m.
F_m= equivalent lateral forces in the *m*th mode, KN.
$H_u(\omega)$ =complex frequency-response function, dimensionless.
I = moment of inertia of the lumped mass, m^4.
J= nodal rotational inertia, Kg m^2.
K= stiffness matrix, N/m.
K_2=loss stiffness, N/m.
K_R=rotational stiffness, N/m.
k_{col}=stiffness of column, N/m.
k_{eq}=equivalent complex stiffness, N/m.
L =floor height, m.
M=mass matrix, Kg.
P_t=complex periodic loading function, KN.
*S*1=mapped MCE, 5 percent damped, spectral response acceleration parameter at a period of 1, %g.
Ss=mapped MCE, 5 percent damped, spectral response acceleration parameter at short periods, %g.
t =core thickness, m.
u= displacement of the system and the damper, m.
$\dot{u}$=velocity of the piston, m/s.
u_o=amplitude of the displacement, m.
V_m=modal base shears, KN.
W_i=the portion of the total gravity load of the structure at level i, KN.
W_m=effective modal gravity load, KN.
Wx=effective seismic weight at each node, KN.
ω=frequency of motion, rad/s.
ω_n =vibration Natural Frequency, rad/s.
δ=phase angle, rad.
ζ =damping ratio, dimensionless.
ζ_{eq} =equivalent damping ratio, dimensionless.
β=rotation of the core, rad.
ϕ=eigenvectors represent the mode shape and the Eigen-values, dimensionless.

ϕ_{im}=displacement amplitude at the *i*th level of the structure when vibrating in its *m*th mode, m.

ϕ_{xm}=displacement amplitude at the *xth* level of the structure when vibrating in its *m*th mode, m.

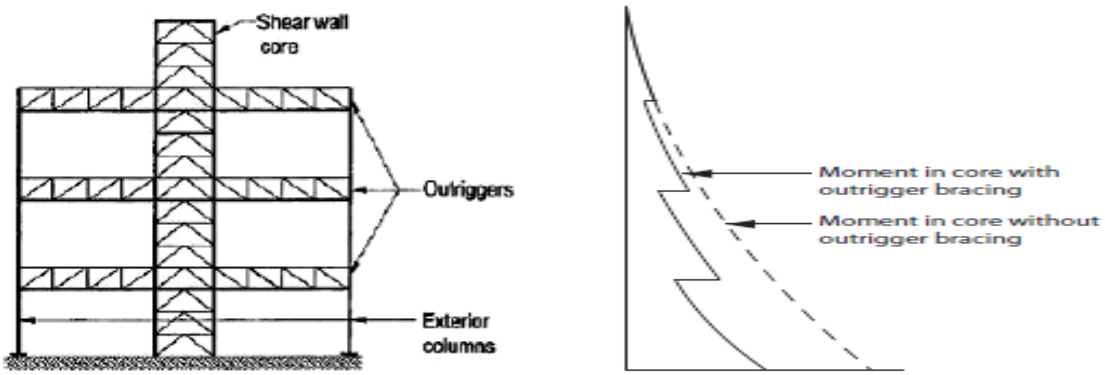

Figure 1. Core – Supported outrigger structures**, Sathyanarayanan, et al., 2012.**

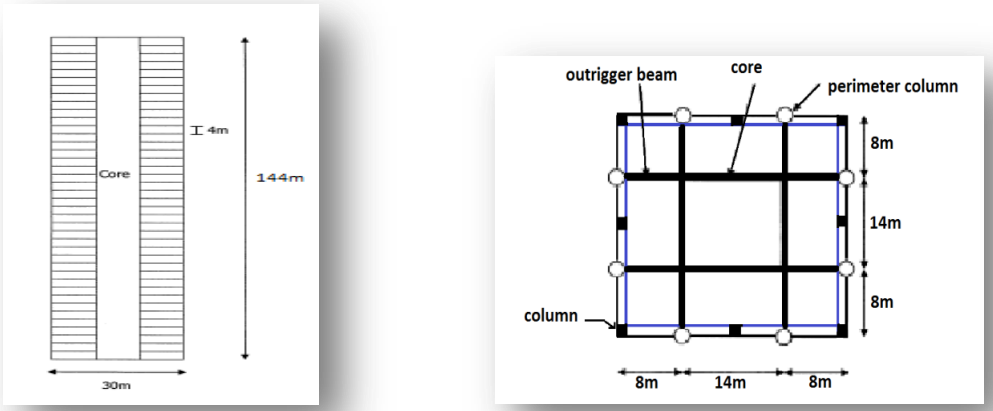

(a) **(b)**

Figure 2. Buildings dimensions (a) in elevation, (b) in plan (some details and beams for gravity system omitted for clarity).

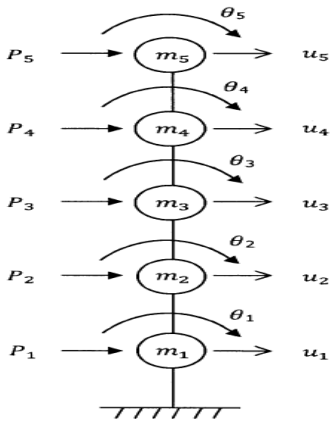

Figure 3. Discrete lumped mass modal for a 5- story building.

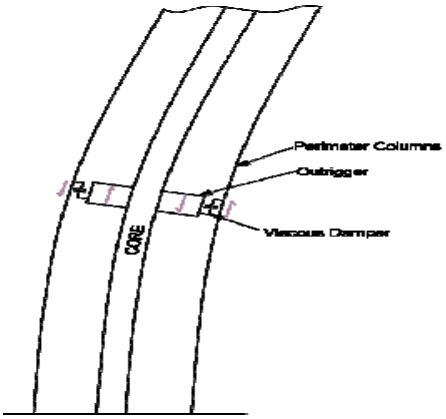

Figure 4. Patent pending (damped outrigger), **Smith, and Willford, 2007.**

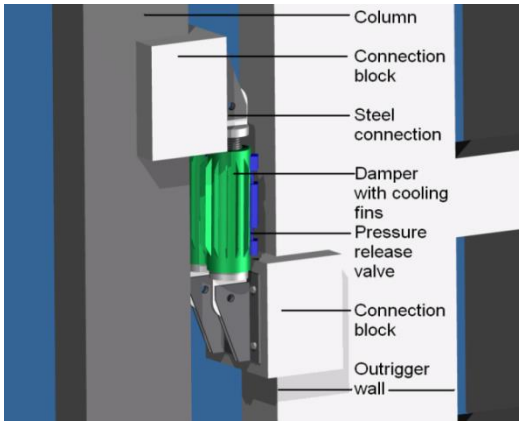

Figure 5. Conceptual detail at outrigger level, **Smith, and Willford, 2007.**

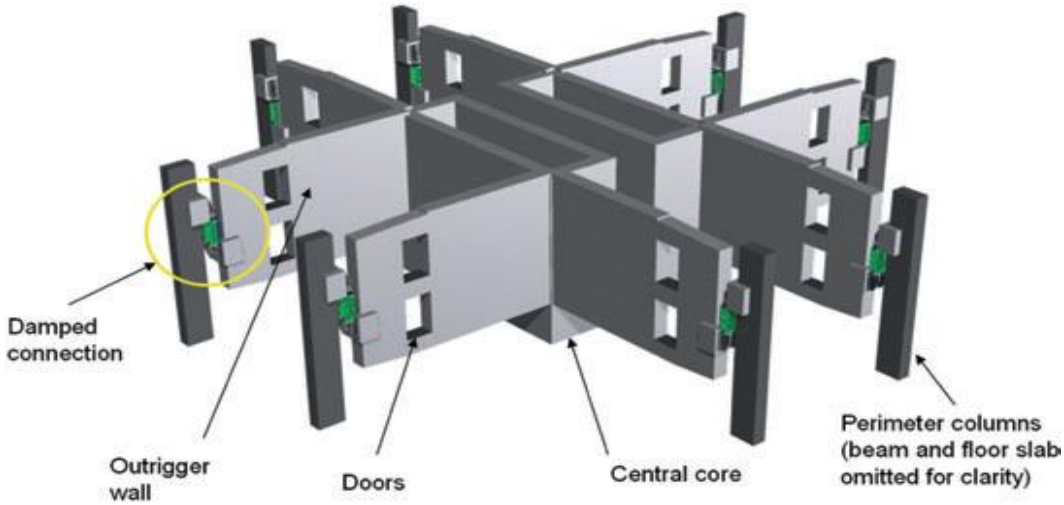

Figure 6. General arrangement of outrigger levels**, Smith and Willford, 2007.**

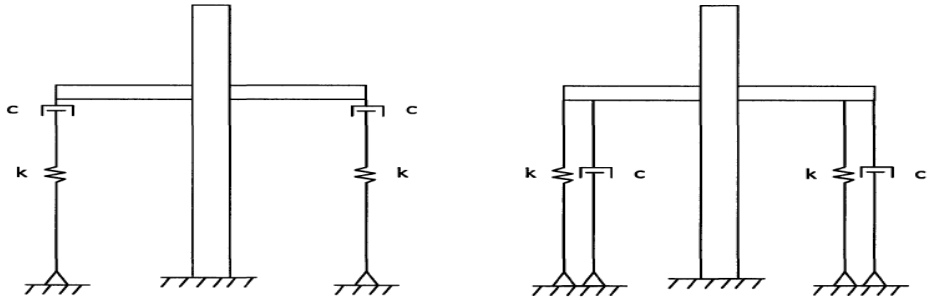

(a) **(b)**

Figure 7. Simplified models of the damped outrigger systems in (a) series (b) parallel**, Gamaliel, 2008.**

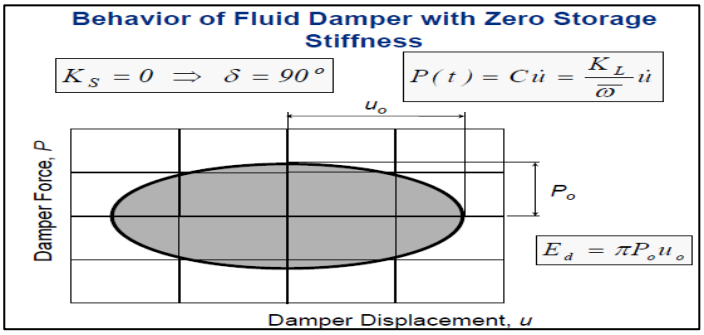

Figure 8. Hysteretic loop for viscous damper.

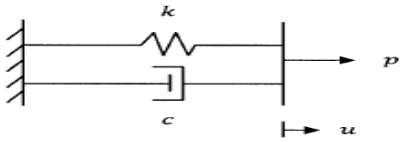

Figure 9. Damper in parallel.

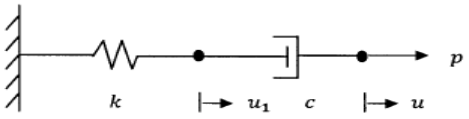

Figure 10. Damper in series.

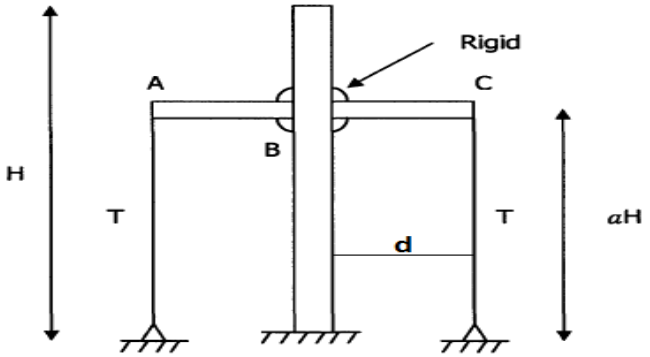

Figure 11. Simplified single outrigger model.

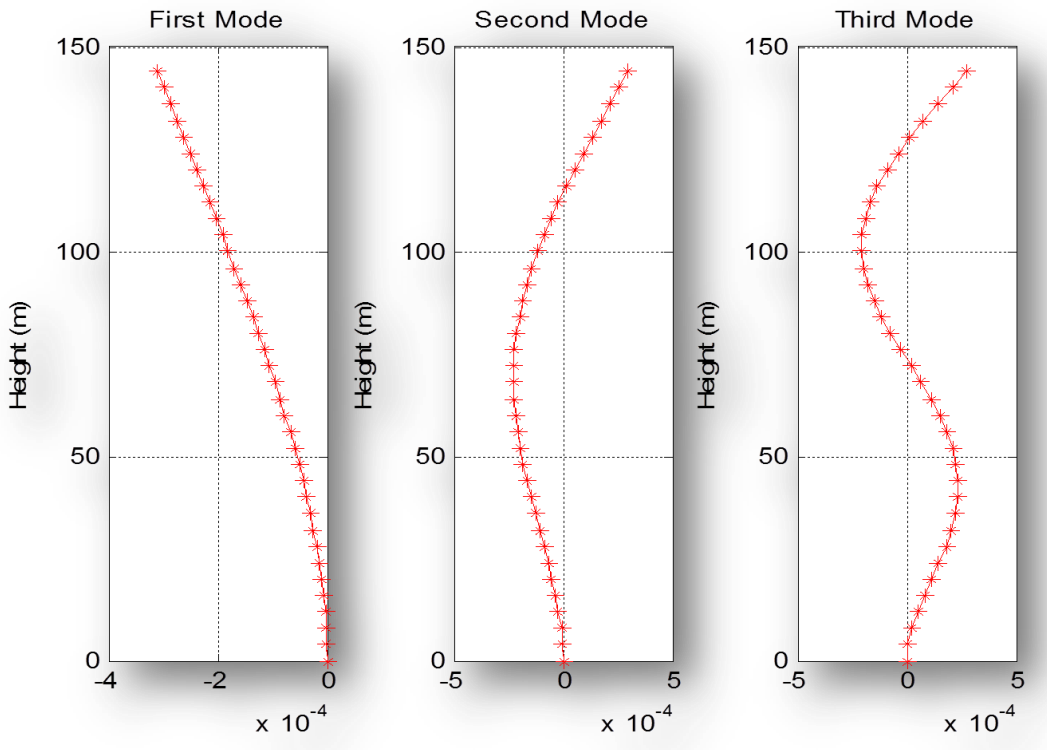

Figure 12. Mode shapes of first three modes for series and parallel system.

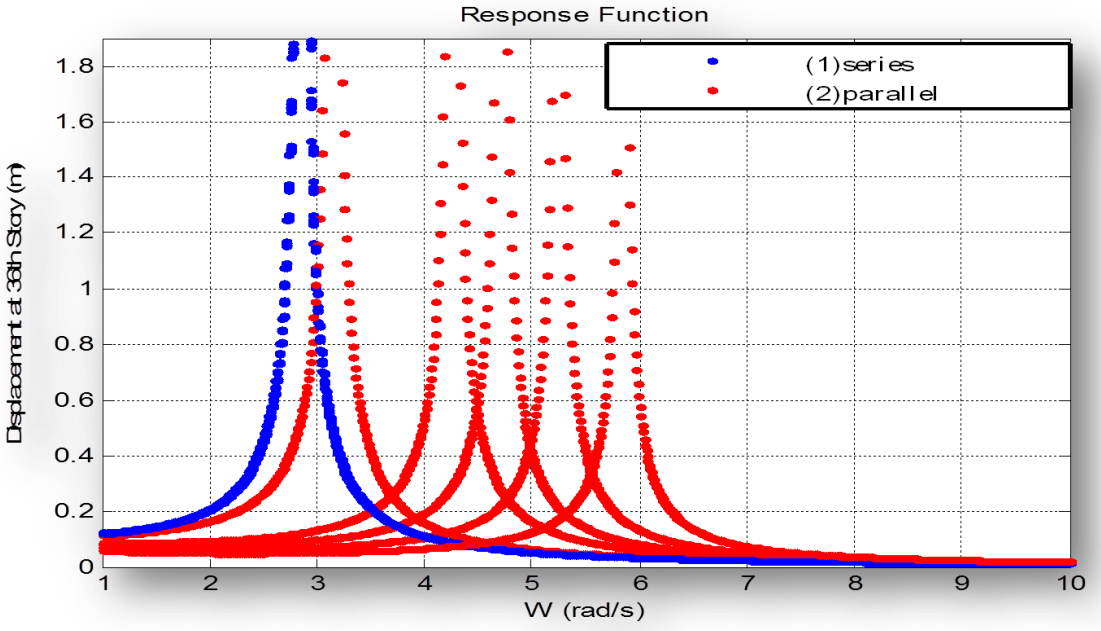

Figure 13. Response function at fundamental mode with different values of damping coefficient, C= 50; 100; 150; 200; 300($MN.S/m$), (horizontal displacement at 36th story **vs** w (rad/seconds)).

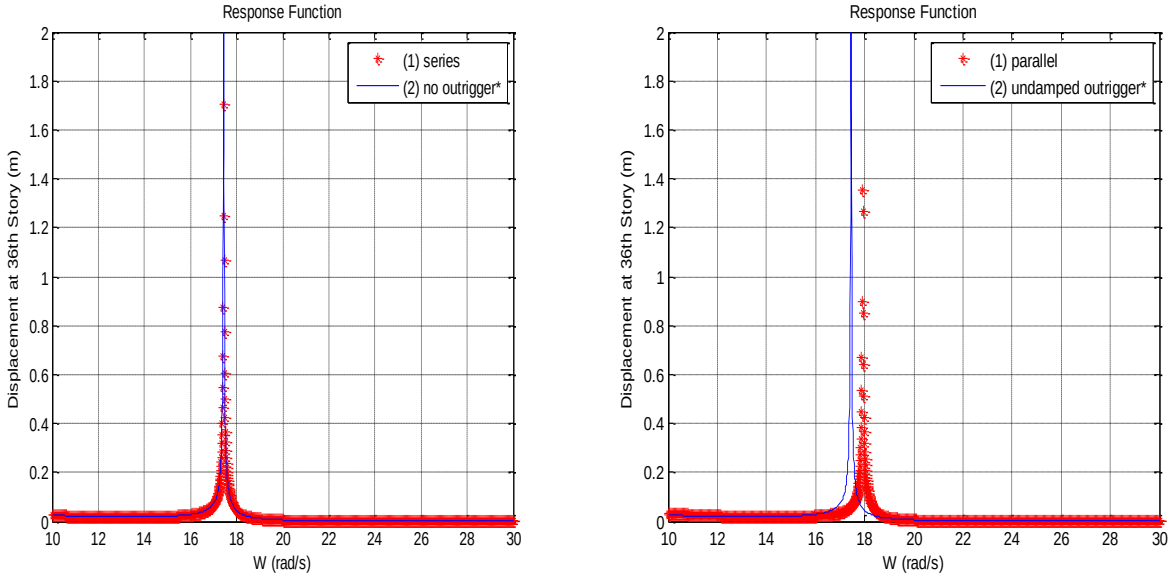

(a)series system (b)parallel system

Figure 14. Frequency-based response function for mode two at C = 100,000 $(KN.S/m)$ (horizontal displacement at 36th story **vs** w (rad⁄seconds)).

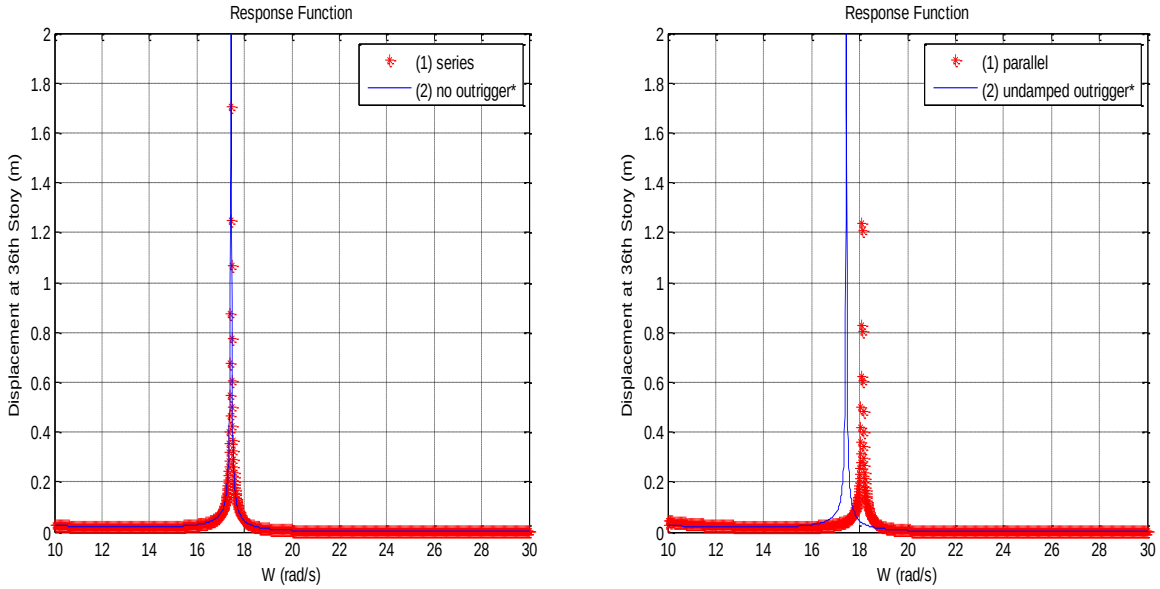

(a)series system (b)parallel system

Figure 15. Frequency-based response function for mode two at C = 200,000 $(KN.S/m)$ (horizontal displacement at 36th story **vs** w (rad⁄seconds)).

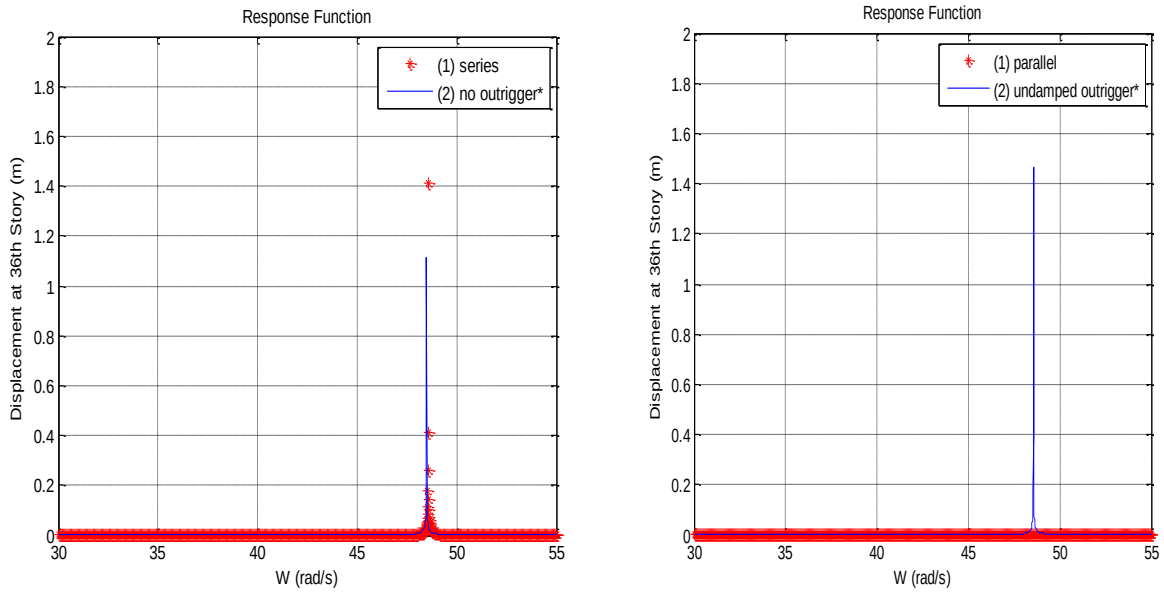

(a)series system (b)parallel system

Figure 16. Frequency-based response function for mode three at C = 100,000 $(KN.S/m)$ (horizontal displacement at 36th story **vs** w (rad⁄seconds)).

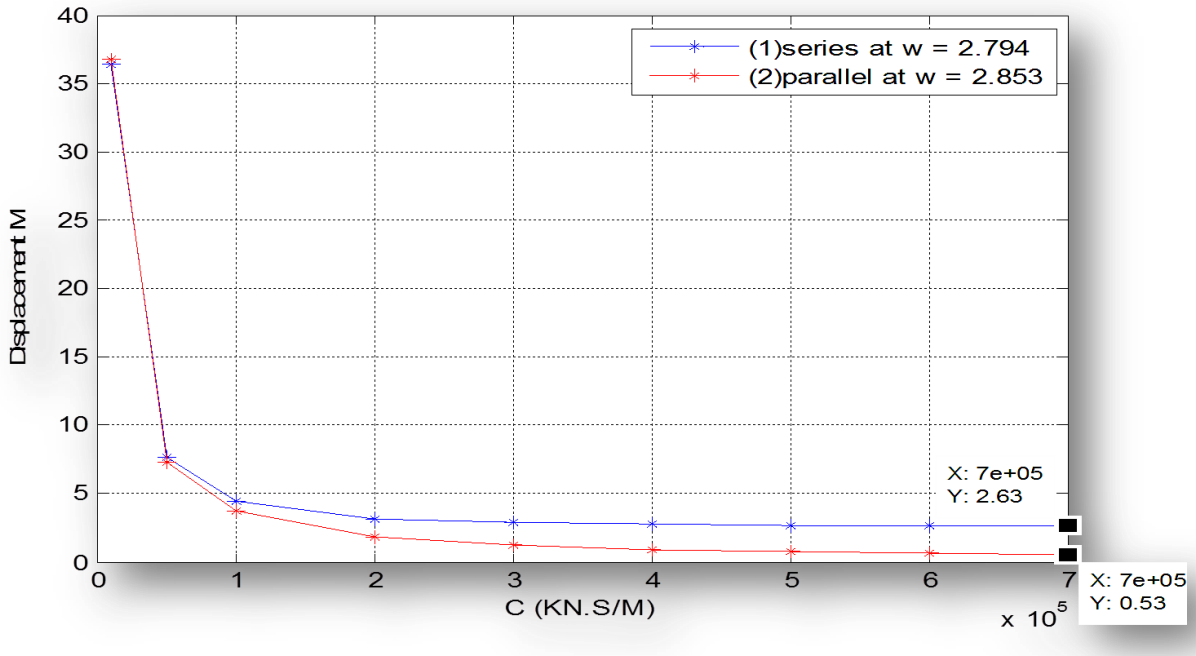

Figure 17. Plot damping coefficient vs displacement at mode one.

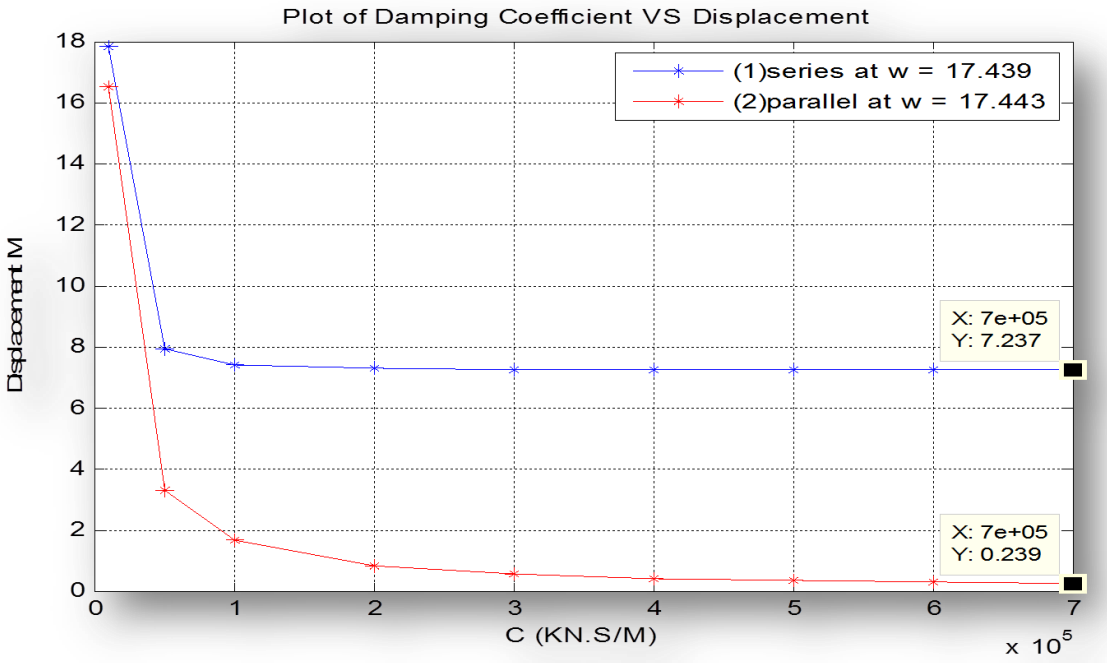

Figure 18. Plot damping coefficient vs displacement at mode two.

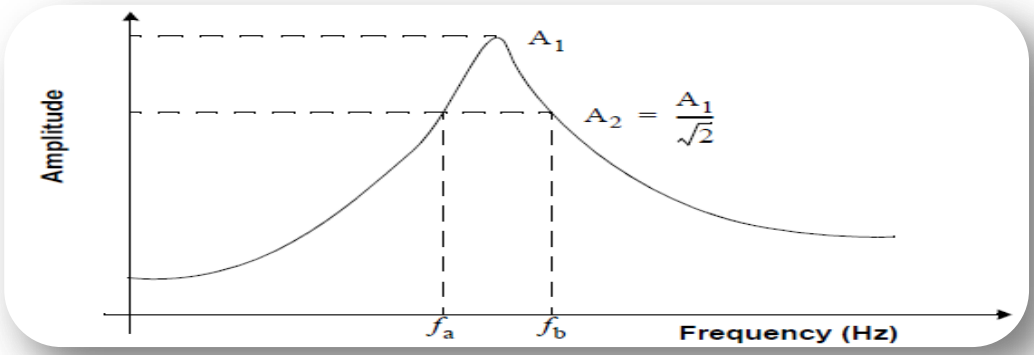

Figure 19. Half power bandwidth method.

Table 1. Frequency and natural periods for series and parallel configuration.

	Mode No.	Frequency (rad / sec)	Period (seconds)
Series configuration	1	**2.794**	**2.246**
	2	**17.439**	**0.3603**
	3	**48.487**	**0.1296**
Parallel configuration	1	**2.853**	**2.2023**
	2	**17.443**	**0.3602**
	3	**48.557**	**0.1294**

Table 2. Modal base shears and equivalent lateral forces for series and parallel configuration.

Mode No.	T_m (seconds)	Sa_m spectral acceleration	CS_m modal coefficient	V_m (*KN*)	Cx_m distribution factor	F_m (*KN*)
1*	2.248	0.2322	0.033	8907	0.0687	611.666
2*	0.3603	0.9840	0.141	11686	0.1175	1373.200
3*	0.1296	0.9840	0.141	4048	0.1903	770.316
1**	2.2023	0.2370	0.034	9104	0.0686	624.735
2**	0.3602	0.9840	0.141	11650	0.1178	1372.700
3**	0.1294	0.9840	0.141	4042	0.1903	768.945

* series configuration

** parallel configuration

Table 3. For mode one (relationship between the C and ξ).

C (KN.s/m)	ξ		% damping	
	series	parallel	series	parallel
10,000	**0.037**	**0.032**	**3.7**	**3.2**
50,000	**0.041**	**0.036**	**4.1**	**3.6**
100,000	**0.044**	**0.042**	**4.4**	**4.2**
150,000	**0.046**	**0.049**	**4.6**	**4.9**
200,000	**0.051**	**0.058**	**5.1**	**5.8**
300,000	**0.054**	**0.066**	**5.4**	**6.6**
400,000	**0.052**	**0.085**	**5.2**	**8.5**
500,000	**0.047**	**0.123**	**4.7**	**12.3**